Phase Separation of Rigid Polymers in Poor Solvents. 1. (Hydroxypropyl)cellulose in Water

C. Lárez-V and V. Crescenzi*

Dipartimento di Chimica, Università La Sapienza, 00185 Roma, Italy

A. Ciferri

Istituto di Chimica Industriale, Università di Genova, 16132 Genova, Italy

Received November 15, 1994; Revised Manuscript Received March 22, 1995®

ABSTRACT: Aqueous solutions of (hydroxypropyl)cellulose, which can be either isotropic (dilute regime) or cholesteric (concentrated regime) at room temperature, exhibit reversible phase separation upon heating above ~37 °C. The biphasic system does not gel and includes a concentrated phase having the appearance of an emulsion of poorly organized microaggregates, and a dilute solution from which the concentrated phase cannot be completely separated. Ellipticity data suggest the onset of cholesteric order at temperatures slightly below those at which isotropic solutions undergo phase separation. This hint of the formation of the mesophase is detected at concentrations unusually low (~0.4% v/v). The conjugation of the two phases was evidenced by determination of the individual volumes and concentrations. The pseudo phase diagram includes boundaries for the high-temperature biphasic region which are not readily interpreted in terms of a heat-induced crystallization process. It is suggested that the primary event controlling phase separation is the driving force for the formation of a mesophase in a solvent which becomes poorer upon increasing temperature ("inverted" wide region of the theoretical diagram). The development of well-organized liquid crystalline domains, and their possible evolution toward a crystalline state, may be greatly slowed down by kinetic effects.

Introduction

The formation of mesophases in solutions of rigid or semirigid macromolecules is primarily controlled by excluded-volume effects, or hard interactions, as expressed by axial ratios and concentration.[1,2] Soft interactions usually play a minor role, and, in fact, the critical concentration is generally small and not much affected by temperature.[3,4] In most cases in which a significant temperature effect was observed, it was attributed to a conformational alteration rather than to intermolecular interaction.[5]

A quite different situation is, however, expected when soft interactions, isotropic in nature, are particularly strong as in the case of a thermodynamically poor solvent for the polymer. Polymer–polymer interactions are then favored, and the critical concentration is largely temperature-dependent and may be pushed down to extremely low concentration with a large widening of the biphasic gap. The effect has been predicted theoretically,[1-4] but its experimental verification is complex and uncertain.[5] Yet, the possibility of forming mesophases at very low polymer concentration appears to have great significance in terms of both self-assembly mechanisms for biological systems and the fabrication of oriented structures for synthetic polymers.[6]

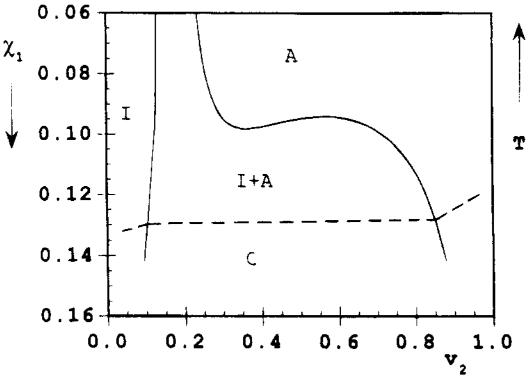

Figure 1. Theoretical phase diagrams for "normal" solutions of monodisperse rodlike molecules ($X = 60$). Calculated from the original 1956 Flory theory. The dashed line represents a crystallization boundary drawn following ref 6.

The theoretical prediction is well-known, and Figure 1 details the wide biphasic gap on a temperature–polymer volume fraction (v_2) diagram calculated from the simplest lattice theory.[1] Although no effects due to polydispersity, partial flexibility, and soft anisotropic attraction are included, the figure clearly shows how the spread between the conjugated concentrations $v_2{}^{i}$ and $v_2{}^{a}$ at which the isotropic and anisotropic phases coexist is altered by temperature. The χ_1 interaction parameter is defined as

$$\chi_1 = {}^1/_2 + (\kappa_1 - \Psi_1) = {}^1/_2 - \Psi_1(1 - \Theta/T)$$

where Θ is the theta temperature while κ_1 and Ψ_1 are the component enthalpy and entropy of dilution parameters, respectively.[7] For instance, for an axial ratio $X = 60$, $v_2{}^{a} \sim 0.27$ in good solvents with low χ_1 (narrow region), while $v_2{}^{a} \sim 0.80$ in poor solvents (wide region). The reduction of $v_2{}^{i}$ in the wide region is even larger ($v_2{}^{i}$ falling below 0.01) if account is taken of partial flexibility and soft anisotropic attractions.[4] Note also the asymmetry of the two curves limiting the biphasic region and the appearance of a second anisotropic phase within the wide region when $X > 50$. Since the wide region occurs on cooling, the case represented in Figure 1 is typical of "normal" systems, with solvent quality decreasing on decreasing temperature, i.e., upper critical solution temperature, when χ_1 decreases with temperature and both Ψ_1 and κ_1 have positive sign. However, one may expect a wide region on heating in the case of "inverted" systems having lower critical solution temperature when χ_1 increases with temperature and

---

® Abstract published in *Advance ACS Abstracts*, June 1, 1995.

0024-9297/95/2228-5280$09.00/0

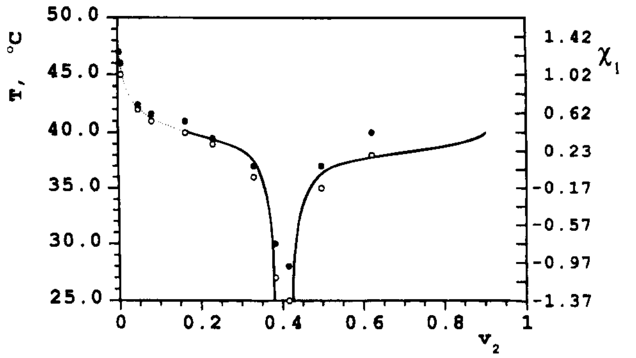

Figure 2. Cloud points for HPC in H_2O *vs* the overall polymer volume fraction v_2: (○) clear monophasic solutions; (●) turbid biphasic mixtures. The full line was calculated from the same theory used in Figure 1, but $X = 22$ and "inverted" systems.

both Ψ_1 and κ_1 have negative sign. One such case ($X = 22$) is included in Figure 2.

The complexity involved in extending the experimental observation of the phase diagram into the wide region is primarily due to the fact that in thermodynamically poor solvents the solubility is low. Even though the critical composition $v_2{}^i$ is lower than in the case of good solvents, the conjugated composition $v_2{}^a$ is so large that its thermodynamically stable state is that of a crystal, rather than a liquid crystal. The encroachment of the equilibria in Figure 1 with a crystallization equilibrium has been theoretically discussed.[6,8,9] In Figure 1 we have sketched a possible crystallization line. For a normal system the crystalline phase is stable at low temperature and may overshadow the wide region. Metastability, or low nucleation rate, may, nevertheless, allow the observation of the conjugated phases.[6,8,9] The system may also enter a non-nucleation kinetic mode (spinodal) before true thermodynamic equilibrium sets in.[10,11] In these cases crystallization will be directed by the liquid crystalline precursor even for very low values of v_2.

Precipitation and, more often, gelation have been in fact observed for most of the mesogenic polymers under situations in which the thermodynamic quality of the solvent is altered by cooling, or by heating, or by solvent composition changes.[8-14] The formation of the gel has been regarded as a manifestation of crystallization in the case of poly(*p*-benzamide) in *N*,*N*-dimethylacetamide/LiCl,[8] as a manifestation of spinodal decomposition of the conjugated phases within the wide region[10,11] in the case of poly(γ-benzyl L-glutamate) (PBLG) in dimethylformamide, and as a manifestation of both spinodal decomposition and crystallization in the case of cellulose in NH_3/NH_4SCN.[12] Gelation driven by a spinodal mode is often manifested by the formation of a bicontinuous phase, and a valid region to calculate a spinodal curve is that where the system separates into two different mesophases. This is expected (cf. Figure 1) only when large axial ratios are considered. Dynamic light scattering analysis of PBLG in several solvents showed how difficult and uncertain is the characterization of gelation in terms of spinodal decomposition.[11]

We have, therefore, analyzed experimental data for a variety of systems, looking for any possible evidence of a wide region uncomplicated by gel formation. In our opinion, the (hydroxypropyl)cellulose (HPC)–water system, recently reinvestigated by Fortin and Charlet,[15] merits additional consideration.

HPC–Water System. The HPC–water system has been extensively investigated dating from the pioneering observation of the occurrence of a cholesteric phase reported by Werbowyj and Gray[16] in 1976. Most of the investigations (reviewed by Fortin and Charlet[15]) emphasize the low-temperature region of the phase diagram where isotropic solutions are stable when v_2 is ≤ 0.38. A mixed isotropic–cholesteric narrow region then appears, and a pure cholesteric phase prevails when $v_2 \geq 0.45$.[15,18] A gel may sometimes be observed in the high-concentration region ($v_2 > 0.8$). The composition–temperature boundaries of the narrow region are not altered in the low-temperature range, but the solutions undergo a reversible phase separation upon heating above ~40 °C, yielding a precipitate consisting of a white concentrated phase mixed with a clear diluted solution.[15] The significance of the heat precipitation was possibly overlooked in early investigations,[18] but Fortin and Charlet analyzed the phenomenon in detail. They concluded that the white phase shows evidence of cholesteric order, it is not gellified, and its emulsion with the diluted solution is stabilized by a decrease of the surface tension of water due to HPC.[17]

From turbidity–temperature data on solutions of known composition, Fortin and Charlet sketched a pseudo phase diagram which is strongly reminiscent of the theoretical diagram in Figure 1. However, the authors described the phase separation at high temperature as a reduced solubility process due to the melting of water structures at high temperature and did not consider a correlation of their diagram with the theoretical wide region of Figure 1. Therefore, we decided to present additional data and considerations intended to complement the excellent work of Fortin and Charlet. The analysis offers support to the identification of the phase separation of HPC in water with the wide region theoretically predicted, uncomplicated by gelation effects.

Experimental Section

Materials. The HPC used was an unfractionated sample (LF) supplied by Hercules Inc., similar to that described in previous publications.[18] Its intrinsic viscosity in EtOH at 25 °C was 1.42 dL/g corresponding[19] to a molecular weight $M_v = 150\,400$ and a degree of polymerization = 355. Molar substitution (MS, average number of moles of propylene oxide per mole of anhydroglucose unit) was on the order of 5[15,19] [greater than 3, the maximum degree of substitution DS, due to the occurrence of oligo(1,2-alkyleneoxy) side chains]. Polymer volume fraction v_2 was calculated using the partial specific volume of HPC in water previously measured[18] (0.833 mL/g) and the specific volume of water. A simple conversion between volume and weight fraction (w_2) is $v_2 \sim 0.89 w_2$. Solutions were prepared by mixing known amounts of HPC and H_2O, stirring, and allowing homogenization at room temperature in closed tubes, removing if necessary air bubbles under moderate vacuum. The most concentrated solution (75% w/w) was prepared by wetting the polymer and homogenizing it before the correct amount of water was added. Since the homogenization process appeared to be very slow at room temperature, it was completed at 45 °C, taking advantage of the reduced bulk viscosity of the system. Final concentrations were confirmed by the dry weight of aliquots from which the solvent was evaporated at 100 °C.

Turbidity and Mesophase Formation. Cloud points were determined by placing glass tubes containing different HPC solutions in a thermostat, allowing at least 1 h of equilibration, and then increasing the temperature by 0.5 °C increments (rate < 1 °C/h). We recorded the maximum temperature at which solutions remained clear and the minimum temperature at which turbidity was visually detectable, comparing with a reference tube containing water. When sufficient turbidity had developed, the temperature was lowered by similar decrements, recording the lowest temperature at which turbidity could be detected. Reproducibility was within 1 °C. In order to separate the coexisting phases, solutions contained in calibrated glass tubes were equilibrated in the thermostat at 62 °C for at least 24 h. NaCl (0.05% w/v) was then added, waiting a few days to optimize phase separation. The clear supernatant phase was separated with a pipette. The concentration of each phase was determined by measuring the rotatory power and comparing it with a calibration curve for HPC in H_2O + NaCl (0.05%) at 25 °C and $\lambda = 365$ nm.

Volumes fractions $\Phi_i = V_{iso}/V_{aniso}$ were deduced from the calibrated tubes. Concentrated solutions were observed at room temperature under a polarizing microscope (Leitz, Ortholux II). For ellipticity measurements we used a Jasco J-500A dichrograph equipped with thermostated cells having a 1 mm optical path designed in our laboratory to handle viscous samples. Measurements of ellipticity were performed for values of the voltage of the detector smaller than 400 V corresponding to clear, nonturbid solutions. Measurements were performed between 350 and 500 nm following the ellipticity as a function of time at a given temperature. When an equilibrium value was reached, the temperature was raised, waiting for another equilibrium value. The average rate of temperature increase was ~2 °C/h. The temperature was eventually lowered, and full reversibility was observed.

Results and Discussion

Cloud temperatures for solutions of known v_2 are plotted in Figure 2. A narrow region at low temperature is bound between temperature-independent values of $v_2^i \sim 0.38$ and $v_2^a \sim 0.42$ with $v_2^a/v_2^i \sim 1.10$. On increasing temperature the biphasic region begins to widen up due to a strong temperature dependence of the critical compositions. Although qualitatively similar to the data reported by Fortin and Charlet for fractioned samples, the present results show a more pronounced temperature dependence of the v_2^i *vs* temperature boundary and a less pronounced asymmetry of the v_2^i *vs* T and v_2^a *vs* T curves. Moreover, both v_2^i and v_2^a are somewhat smaller than the values reported by the latter authors, even allowing for their use of weight fractions. They have already discussed differences of this type which may be due to differences in molecular weight distribution, DS, MS, and Mv.

The full lines in Figure 2 represent a theoretical diagram calculated from the theory of monodisperse rods[2] having $X = 22$. The calculation is performed to the limiting value $\chi_1 \sim 0.5$, at which calculation shows that the system reaches full orientation (order parameter $y = 1$).[2] The good fit between theory and experiment suggests that $T \sim 41$ °C corresponds to $\chi_1 \sim 0.5$ ($T = \Theta$). The theoretical line can therefore represent only the onset of the wide region, while the upper part of the wide region cannot be represented by this theory. In fact, one might be surprised by the ability of the theory valid for monodisperse rods to represent both the narrow region and the onset of the wide one. HPC is a semirigid chain with persistence length q varying from 70 to 100 Å depending upon the solvent.[5,23] The relevant axial ratio to be used in connection with theories for semirigid chains[4,5,20] is $X = 2q/d$ (d is the chain diameter) independent of molecular weight. Taking for HPC in H_2O $q = 85$ Å and an axial ratio $X = 17$, the critical volume fraction calculated for the Kuhn chain model[4,5,20] in the narrow region is $v_2^i \sim 6.7/X = 0.39$. This figure is very close to the experimental value in Figure 2 and, moreover, is also close to the value calculated from the theory used in Figure 2 ($v_2^i \sim 6.4/X = 0.38$). Since $d \ln q/dT$ is on the order[5,23] of -5×10^{-3} deg^{-1}, a small reduction of q from 25 to 41 °C is expected, but this decrease is certainly inadequate to justify the occurrence of a conventional liquid–liquid separation such as that observed for flexible polymers.

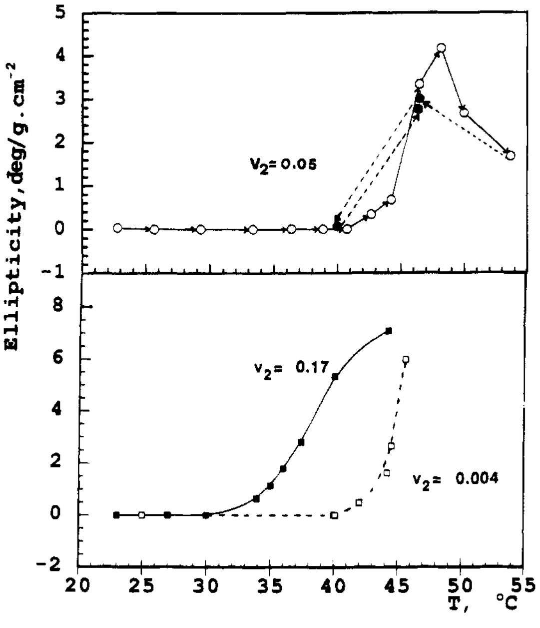

Figure 3. Ellipticity–temperature data for HPC in H_2O at the indicated v_2. Rate of temperature increase is ~2 °C/h. $\lambda = 460$ nm for $v_2 = 0.05$; $\lambda = 500$ nm for $v_2 = 0.17$.

The cholesteric nature of the concentrated monophasic and of the biphasic solutions at room temperature was confirmed by detection, under the polarizing microscope, of the typical fingerprint pattern. Typical ellipticity–temperature curves for solutions which were isotropic at room temperature are shown in Figure 3. The helicoidal arrangement of the molecules causes the reflection of one component of circularly polarized light,[16] and ellipticity has been taken as an indication of the mesophase.[15,16] Under the extremely low rate of temperature increase adopted, an increase of ellipticity is observed even before turbidity is detected. When turbidity is appreciable, ellipticity starts to decrease and the microscope observation cannot be performed. A difference of only about 2 °C on the transition temperatures deduced from Figures 2 and 3 is noticeable. This small difference between the two measurements supports the reliability of the pseudo phase diagram in Figure 2. Since the onset of cholesteric order is evident at or just before turbidity appears, the formation of the mesophase seems to be the primary controlling event of the phase separation.

We next analyzed the conjugation of the coexisting phases in the temperature range above 41 °C which is outside the range where comparison with theory (Figure 2) can be made. It is recalled that within the narrow region, when theory can be applied, the volume of the two phases obeys the lever rule and the composition of coexisting phases should be invariant with respect to the overall composition. The latter expectation is strictly valid for a monodisperse system of rodlike molecules.[20,21] However, fractionation effects are expected for polydisperse rods and Kuhn chains but should not be large[4,5] for a wormlike polymer since the axial ratio is controlled by the persistence length and not by the contour length of the molecule.

Attempts to separate the two coexisting phases at temperatures above 40 °C by centrifugation were, however, discouraging. As reported by Fortin and Charlet, the whitish concentrated phase which can be

Table 1. Volume and Composition of Conjugated Phases at 62 °C

overall	isotropic		concentrated	
v_2	Φ_i	v_2^i	$1 - \Phi_i$	v_2^a
0.0042	0.975	0.0008	0.025	0.1263
0.0505	0.775	0.0044	0.225	0.2229
0.1546	0.537	0.0105	0.463	0.4999
0.2447	0.375	0.0206	0.625	0.4394
0.3571	0.185	0.0247	0.850	0.4497

separated from a clear diluted solution is neither a gel nor a pure phase. Volumes and composition of the phases appeared to vary with the extent of centrifugation. The addition of isobutyl alcohol (~7% v/v) had the effect of lowering the phase separation to room temperature, thus allowing more extensive centrifugation. Still, no satisfactory isolation of the concentrated phase was achieved. Eventually, we devised the expedient of adding traces of NaCl (0.05% w/v) directly to the biphasic solution at high temperature. The addition of traces of the salt greatly reduced (but did not completely eliminate) the extent of emulsion and the milky appearance of the concentrated phase. A clearer boundary between the two phases was now evident, and the supernatant isotropic solution could be isolated.

Volume and composition of the isolated phases at 62 °C are reported in Table 1 and in Figure 4 for different values of the overall composition v_2. The data support a tendency toward the conjugation of the two phases. Extrapolation of the overall composition v_2 *vs* the volume fraction of the isotropic phase Φ_i has been used for a reliable determination of the width of the narrow region.[5,22] The extrapolation in Figure 4 (cf. refs 5 and 22) suggests $v_2^i \sim 0.001$ and $v_2^a \sim 0.60$ at 62 °C. While these data are consistent with the results in Figure 2, the value of v_2^a obtained from Figure 4 is likely a lower limit since it is quite possible that the v_2 *vs* Φ_i curve has a still larger upward slope[22] when $\Phi_i \to 0$. Moreover, the concentrated phase still includes some isotropic solution, an effect which also contributes to the observation that the composition of each phase changes with the overall composition. The v_2^a/v_2^i ratio deduced from the above results is surprisingly large, but not in disagreement with theoretical diagrams such as those reported by Khokhlov (see Figure 6 of ref 4) which include a small degree of anisotropic attractions. Moreover, as earlier suggested by Flory[2] occurrence of crystallization (as indicated in Figure 1) could cause an additional alteration of the conjugated concentrations.

To assess kinetics and reversibility, temperature cycles were performed on the whole solutions and on each of the conjugated phases. The whole isotropic and anisotropic solutions at room temperature became turbid as soon as thermal equilibrium was established at a temperature above 40 °C, when the point representative of the system moves inside the wide region and the other phase is formed. Turbidity disappears promptly upon returning the solution to room temperature. Clear isotropic solutions, isolated at a given temperature (>40 °C) from the conjugated phase, develop turbidity upon increasing temperature but remain clear if temperature is lowered to room temperature. The increase of turbidity upon increasing temperature is attributed, in this case, to the fact that the point representative of the solution moves upward from the equilibrium line to a location inside the wide region with further production of the mesophase. An opaque biphasic solution in the narrow region at room temperature develops, reversibly, additional turbidity if temperature is increased. Finally, an anisotropic solution isolated at a given temperature (>40 °C) from the isotropic one still exhibits some turbidity. This turbidity is, however, reduced when temperature is decreased, and the point representative of the system, close to the equilibrium line, moves to a location inside the narrow region. No alterations are evident in the appearance of all solutions if standing periods of a few months are allowed. These observations are not inconsistent with the behavior expected in the wide region and reveal a fast kinetic mechanism for the development and the disappearance of the anisotropic phase which may correspond, or simulate, thermodynamic equilibrium.

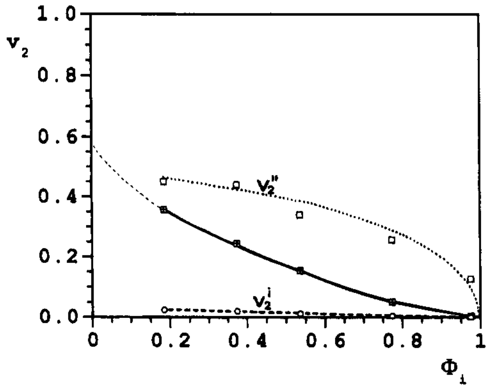

Figure 4. Variation of volume and composition of isotropic and anisotropic phases coexisting at 62 °C for biphasic mixtures of HPC in H_2O with the overall polymer volume fraction. Data from Table 1.

Since the axial ratio of HPC is rather small, we are definitively in the range where two anisotropic phases (cf. Figure 1) cannot be stable. The calculation of the spinodal between two unlike phases would require attempting to differentiate over the discontinuity represented by the narrow region. This difficulty might imply that spinodal decomposition effects giving rise to gelation, as reported for PBLG, are unlikely for the present system. However, Kyu *et al.*[24] studied the phase separation of HPC in water using a time-resolved light scattering setup. While they did not report gelation, they suggested that the phase separation still occurs via spinodal decomposition rather than via nucleation and growth. In fact, HPC solutions at 45 °C and $v_2 \sim 0.10$ developed a scattering halo with the V_v but not with the H_v component of polarized light, indicating a prevalence of concentration over orientation fluctuations. By contrast, the H_v scattering image at room temperature exhibited definite patterns when $v_2 > 0.4$, suggesting the evolution of liquid-crystalline and crystalline domains. However, the early stages of the decomposition were not entirely consistent with the linear Cahn–Hilliard regime, while more recent theories for spinodal decomposition of rodlike polymers are still untested.[25]

Alternative interpretations for the failure to detect clearcut liquid-crystalline or crystalline domains above the phase-separation temperature should be considered. The competition between phase separation and gelation has been recently considered by Tanaka and Stockmayer[26] in the case of junctions with variable multiplicity (e.g., dipole, hydrogen bond aggregation). Topological interferences within the pregel regime clusters could greatly slow down their evolution toward well-organized liquid-crystalline domains, precursors[6] of a crystalline organization. Khoklov[27] has been recently considering the possibility of transitions "arrested" due to kinetic problems. Formation of folded, globular structures significantly below the Θ temperature has been postulated even for wormlike polymers.[28]

Guido[29] has recently presented a study of the morphology of the high-temperature phase of HPC in water using video-enhanced contrast microscopy which allows the attainment of the theoretical resolution of the optical microscope. He was able to detect the faint appearance of maltese crosses within droplets of the concentrated phases, suggesting a slow evolution toward a crystalline organization. The technique is now being applied to the study of the precursor phases close to the equilibrium line, or within the pretransitional range.

Since phase separation occurs on heating, the system exhibits the thermodynamics of an inverted system.[30] We can expand these considerations to investigate the possibility of an underlying crystallization mechanism controlling the phase separation. In the majority of cases, melting occurs on heating and the melting temperature T_m decreases with increasing dilution, i.e., $\partial T_m/\partial v_1 < 0$ and $\partial T_m/\partial v_2 > 0$. This is the normal behavior (M^+ in the terminology of Orofino *et al.*[30]) which requires the total heat involved ($\Delta H = \Delta H_{\mathrm{melting}} + \Delta H_{\mathrm{dilution}}$) to be a positive quantity. The inverted (M^-) behavior occurs when ΔH_{tot} is negative due to the prevalence of a negative heat of dilution. In this case T_m must increase with decreasing polymer concentration, i.e., $\partial T_m/\partial v_1 > 0$ and $\partial T_m/\partial v_2 < 0$. The slopes of the left- and right-hand boundaries of the wide region on the pseudo phase diagram in Figure 2 should correspond, if melting prevailed, to the situations $\partial T_m/\partial v_2 < 0$ and $\partial T_m/\partial v_2 > 0$, respectively. The former is the condition for M^- and the latter for M^+ behavior. However, experimentally, the phase transition is observed on heating on the whole composition range of the wide region. Therefore, while crystallization of the precipitated phase may eventually prevail, the measured phase boundaries in Figure 2 are more consistent with the wide region than with a direct crystallization mechanism.

A final comment concerns the asymmetry of the left- and right-hand boundaries of the biphasic region. Anisotropic solutions appear to phase separate at lower temperatures than isotropic ones. Fortin and Charlet reported a difference as large as 28 °C. The effect is seen here only as a slightly larger curvature for the right than for the left-hand boundary. An asymmetry of the two boundaries is often visible in theoretical diagrams[4,31] and is affected by parameters such as the axial ratio, molecular weight distribution, and partial rigidity. Possibly, another way to describe it could be the introduction of different χ_1 parameters for the two phases (i.e., $\chi_1{}^{\mathrm{i}} < \chi_1{}^{\mathrm{a}}$ in the case of Figure 1). Fortin and Charlet's suggestion that HPC displays a more hydrophobic surface to the solvent in the anisotropic than in the isotropic phase would be described by the above approach.

The observation that liquid-crystalline order might be formed out of a very diluted polymer solution in poor solvents, even if under metastable conditions, has far-reaching significance which will be considered in future work. The attainment of the large concentrations at which liquid crystallinity is commonly observed is often problematic due to the limited solubility of semirigid polymers. These high concentrations might not be attained even in biological fluids out of which ordered structures are formed. One alternative possibility would be an open system where the small amount of mesophase obtained from a diluted solution in a poor solvent could be continuously separated while the overall concentration is kept constant. It should be useful to reanalyze heat precipitation effects reported for other semirigid polymers, for instance, tropocollagen and poly(L-proline) in salt solutions for which a related controversy occurred some time ago.[32,33]

Acknowledgment. C.L.V., on leave from the Universidad de los Andes, Mérida, Venezuela, acknowledges with gratitude support from the JEPA Foundation. The authors express their appreciation to Prof. A. R. Khoklov for critically reading the manuscript.

References and Notes

(1) Onsager, L. *Ann. N.Y. Acad. Sci.* **1949**, *51*, 627.

(2) Flory, P. J. *Proc. R. Soc. London,* Ser. A **1956**, *73*, 234.

(3) Warner, M.; Flory, P. J. *J. Chem. Phys.* **1980**, *73*, 6327.

(4) Khokhlov, A. R. *Liquid Crystallinity in Polymers*; Ciferri, A., Ed.; VCH Publ.: New York, 1991.

(5) Ciferri, A. *Liquid Crystallinity in Polymers*; Ciferri, A., Ed.; VCH Publ.: New York, 1991.

(6) Ciferri, A.; Krigbaum, W. R. *Gazz. Chim. Ital.* **1986**, *116*, 529; *Mol. Cryst. Liq. Cryst.* **1981**, *69*, 273.

(7) Flory, P. J. *Principles of Polymer Chemistry*; Cornell University Press: Ithaca, NY, 1953.

(8) Balbi, A.; Bianchi, E.; Ciferri, A.; Tealdi, A.; Krigbaum, W. R. *J. Polym. Sci., Polym. Phys.* **1980**, *18*, 2037.

(9) Papkov, S. P. *Contemporary Topics in Polymer Science*; Pierce, E. M., Schaefgen, J. R., Eds.; Plenum Press: New York, 1977; Vol. 2; *Polym. Sci. USSR* **1984**, *25*, 1210.

(10) Russo, P. S.; Miller, W. G. *Macromolecules* **1984**, *17*, 1324.

(11) Russo, P. S.; Chodhury, A. H.; Mustafa, M. *Material Research Society Symposium Proceedings*; Adams, W. W., Eby, R. K., McLemore, D. E., Eds.; Materials Research Society: Pittsburgh, PA, **1989**; Vol. 134.

(12) La Marre, C. R.; Cuculo, J. A.; Hudson, S. M.; Ciferri, A. *Mol. Cryst. Liq. Cryst. Lett.* **1991**, *7*, 193.

(13) Bianchi, E.; Ciferri, A.; Conio, G.; Marsano, E. *Mol. Cryst. Liq. Cryst. Lett.* **1990**, *7*, 111.

(14) Ritchey, A. M.; Gray, D. G. *Biopolymer* **1988**, *27*, 1999.

(15) Fortin, S.; Charlet, G. *Macromolecules* **1989**, *22*, 2286. Robitaille, L.; Turcotte, N.; Fortin, S.; Charlet, G. *Macromolecules* **1991**, *24*, 1413.

(16) Werbowyj, R. S.; Gray, D. G. *Macromolecules* **1980**, *13*, 69; **1984**, *17*, 1512.

(17) Chang, S. A.; Gray, D. J. *Colloid Interface Sci.* **1978**, *67*, 579.

(18) Conio, G.; Bianchi, E.; Ciferri, A.; Tealdi, A.; Aden, M. A. *Macromolecules* **1983**, *16*, 1264.

(19) Wirick, M. G.; Waldam, H. H. *J. Appl. Polym. Sci.* **1970**, *14*, 579.

(20) Flory, P. J. *Macromolecules* **1978**, *11*, 1141.

(21) Matheson, R. R.; Flory, P. J. *Macromolecules* **1981**, *14*, 954.

(22) Marsano, E.; Conio, G.; Ciferri, A. *Mol. Cryst. Liq. Cryst.* **1988**, *154*, 69.

(23) Brelsford, G. L.; Krigbaum, W. R. *Liquid Crystallinity in Polymers*; Ciferri, A., Ed.; VCH Publ.: New York, 1991.

(24) Kyu, T.; Zhuang, P.; Mukherjee, P. *Polymer Association Structures*; El-Nokaly, M. A., Ed.; ACS Symposium Series 384; American Chemical Society: Washington, DC, 1989.

(25) Shimada, T.; Doi, M.; Okano, K. *J. Chem. Phys.* **1988**, *88*, 7181.

(26) Tanaka, F.; Stockmayer, W. H. *Macromolecules* **1994**, *27*, 3943.

(27) Khoklov, A. R. Personal communication.

(28) Khoklov, A. R.; Semenov, A. N. *J. Stat. Phys.* **1985**, *38*, 161.

(29) Guido, S. *Macromolecules*. Submitted.

(30) Orofino, T. A.; Ciferri, A.; Hermans, J. J. *Biopolymers* **1967**, *5*, 113.

(31) Abe, A.; Ballauff, M. *Liquid Crystallinity in Polymers*; Ciferri, A., Ed.; VCH Publ.: New York, 1991.

(32) Ciferri, A.; Orofino, T. A. *J. Phys. Chem.* **1966**, *70*, 3277; **1967**, *71*, 1165.

(33) Mandelkern, L.; Liberman, M. H. *J. Phys. Chem.* **1967**, *71*, 1264.

MA946198N